An Algorithm for Stabilization of Fractional-Order Time Delay Systems Using Fractional-Order PID Controllers

Serdar Ethem Hamamci

***Abstract*—This technical note presents a solution to the problem of stabilizing a given fractional-order system with time delay using fractional-order $\mathrm{PI}^{\lambda}\mathrm{D}^{\mu}$ controllers. It is based on determining a set of global stability regions in the (k_p, k_i, k_d)-space corresponding to the fractional orders λ and μ in the range of (0, 2) and then choosing the biggest global stability region in this set. This method can be also used to find the set of stabilizing controllers that guarantees prespecified gain and phase margin requirements. The algorithm is simple and has reliable result which is illustrated by an example, and, hence, is practically useful in the analysis and design of fractional-order control systems.**

***Index Terms*—Fractional-order PID controller, fractional-order systems, gain and phase margins, stabilization, time delay.**

I. Introduction

The PID controller is unquestionably the most commonly used control algorithm in the control industry [1]. The primary reason is its relatively simple structure that can be easily understood and implemented so that many sophisticated control strategies, such as model predictive control, are based on it. Over the last half-century, a great deal of academic and industrial effort has focused on PID control, mainly in the areas of tuning rules, identification schemes, and stabilization methods (see, e.g. [1]–[3], and references therein). In recent years, considerable attention has been paid to control systems whose processes and/or controllers are of fractional-order. This is mainly due to the fact that many real physical systems are well characterized by fractional-order differential equations, i.e., equations involving noninteger-order derivatives [4]. Therefore, to enhance the robustness and performance of PID control systems, Podlubny has proposed a generalization of the PID controllers, namely $\mathrm{PI}^{\lambda}\mathrm{D}^{\mu}$ controllers, including an integrator of order λ and differentiator of order μ (the orders λ and μ may assume real noninteger values) [5]. Various design methods on the $\mathrm{PI}^{\lambda}\mathrm{D}^{\mu}$ controllers have been presented in [5]–[8]. It has been shown in these methods that the $\mathrm{PI}^{\lambda}\mathrm{D}^{\mu}$ controller, which has extra degrees of freedom introduced by λ and μ, provides a better response than the integer-order PID controllers when used both for the control of integer-order systems [6], [7] and fractional-order systems [5], [8]. In these studies, however, very little work is related to the control of fractional-order systems with time delay [4], [9]. Especially, due to the actuator limitations in some systems such as motion control, it is reported in [9] that the system can be well modeled with fractional-order open-loop transfer function with time delay. To the best knowledge of author, the control problem of these systems has not studied for the $\mathrm{PI}^{\lambda}\mathrm{D}^{\mu}$ controllers.

Since the minimal requirement for the controllers is to make the system stable, it is desirable to know the complete set of stabilizing PID parameters for a given plant before controller design and tuning. Many important results have been recently reported on computation of all stabilizing PID controllers for the linear, time-invariant systems with time delay [10]–[13]. However, the stabilization problems considered in these methods completely deal with system's dynamics whose behavior are described by integer-order differential equations. No systematic study currently exists for obtaining the stability regions of the fractional-order systems with time delay using the fractional-order controllers. The formulation, numerical scheme and numerical results for the computation of stabilizing fractional-order $\mathrm{PI}^{\lambda}\mathrm{D}^{\mu}$ controllers for the fractional-order time delay systems presented in this paper are attempts to fill this gap.

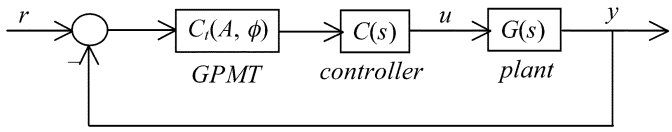

Fig. 1. A general SISO fractional-order control system structure.

In this note, the results of D-decomposition method [14]–[17] which has been widely applied to the parameter space design of fixed-structure controllers [18], [19] for the integer-order systems are generalized to the case of fractional-order $\mathrm{PI}^{\lambda}\mathrm{D}^{\mu}$ controllers $C(s) = k_p + (k_i/s^{\lambda}) + k_d s^{\mu}$ that stabilize a given fractional order system with time delay. The solution to the $\mathrm{PI}^{\lambda}\mathrm{D}^{\mu}$ stabilization problem presented here is based on first obtaining the global stability region for the fixed values of λ and μ in the (k_p, k_i, k_d)-space by using the stability domain boundaries. To achieve this, analytical and straightforward expressions for describing the stability boundaries are derived. Then, for the range of (0, 2) of λ and μ, a set of global stability regions are computed. Finally, the biggest global stability region which has naturally the most various behaviors of the control system in this set is plotted. The final step is necessary because the plotting of complete stability region including all stabilizing $\mathrm{PI}^{\lambda}\mathrm{D}^{\mu}$ controllers is difficult since the $\mathrm{PI}^{\lambda}\mathrm{D}^{\mu}$ controller has five parameters. The presented method is also used for computation of $\mathrm{PI}^{\lambda}\mathrm{D}^{\mu}$ controllers for achieving user specified gain and phase margins for the fractional-order time delay systems. Furthermore, this approach provides several considerable advantages such as it can be applied to the fractional-order time delay systems with parametric uncertainties and also fractional-order chaotic systems with time delay.

II. $\mathrm{PI}^{\lambda}\mathrm{D}^{\mu}$ Control System for Fractional-Order Time Delay Systems

Consider a fractional-order control system to be used in this paper shown in Fig. 1 where $G(s)$ is the fractional-order time delay system, $C(s)$ is the fractional-order $\mathrm{PI}^{\lambda}\mathrm{D}^{\mu}$ controller and $C_t(A, \phi)$ is the gain-phase margin tester. In the practical control systems, the block of $C_t(A, \phi)$ is nonexistence. It is only used for the analysis or design of the $\mathrm{PI}^{\lambda}\mathrm{D}^{\mu}$ controllers.

Definition 2.1: A *fractional-order time delay system* (FOTDS) is defined by the dynamic system represented by the fractional-order transfer function with time delay where the orders of derivatives can take any real number, not necessarily integer number. Consider the transfer function of the FOTDS given as the following expression:

$$\begin{aligned} G(s) &= \frac{N(s)}{D(s)} \\ &= \frac{b_n s^{\beta_n} + b_{n-1} s^{\beta_{n-1}} + \ldots\ldots\ldots + b_1 s^{\beta_1} + b_0 s^{\beta_0}}{a_n s^{\alpha_n} + a_{n-1} s^{\alpha_n - 1} + \ldots\ldots\ldots + a_1 s^{\alpha_1} + a_0 s^{\alpha_0}} e^{-\theta s} \\ &= \left(\sum_{i=0}^{n} b_i s^{\beta_i} \Big/ \sum_{i=0}^{n} a_i s^{\alpha_i} \right) e^{-\theta s} \end{aligned} \tag{1}$$

Manuscript received May 26, 2006; revised December 4, 2006 and May 26, 2007. Recommended by Associate Editor X. Xie.

The author is with the Electrical-Electronics Engineering Department, Inonu University, 44280 Malatya, Turkey (e-mail: shamamci@inonu.edu.tr).

Color versions of one or more of the figures in this paper are available online at http://ieeexplore.ieee.org.

Digital Object Identifier 10.1109/TAC.2007.906243

where θ is the time delay, $a_i, b_i, \beta_n > \ldots\ldots > \beta_1 > \beta_0 \geq 0$ and $\alpha_n > \ldots\ldots > \alpha_1 > \alpha_0 \geq 0$ are arbitrary real numbers. In the time domain, $G(s)$ corresponds to the $(n+1)$-terms inhomogeneous fractional-order differential equation

$$\sum_{i=0}^{n} a_i D^{\alpha_i} y(t) = \sum_{i=0}^{n} b_i D^{\beta_i} u(t-\theta) \tag{2}$$

where $y(t)$ is the output and $u(t)$ is the input of the plant of (1).

Definition 2.2: A *fractional-order $PI^{\lambda}D^{\mu}$ controller* (FOPID) can be considered as the generalization of the conventional PID controllers because of involving an integrator of order λ and a differentiator of order μ. The transfer function of the FOPID controller has the form

$$C(s) = \frac{U(s)}{E(s)} = k_p + \frac{k_i}{s^{\lambda}} + k_d s^{\mu} \quad (0 < \lambda, \mu < 2). \tag{3}$$

Taking $\lambda = 1$ and $\mu = 1$ in (3), it is obtained a classical PID controller. $\lambda = 1$ and $\mu = 0$ give a PI controller, $\lambda = 0$ and $\mu = 1$ give a PD controller, and $\lambda = 0$ and $\mu = 0$ give a gain.

One of the most important advantages of the $\mathrm{PI}^{\lambda}\mathrm{D}^{\mu}$ controller is the possible better control of fractional-order dynamical systems. Another advantage lies in the fact that the $\mathrm{PI}^{\lambda}\mathrm{D}^{\mu}$ controllers are less sensitive to changes of parameters of a controlled system [5]. This is due to the two extra degrees of freedom to better adjust the dynamical properties of a fractional-order control system.

Definition 2.3: A *gain-phase margin tester* (GPMT), can be thought of as a "virtual compensator," provides information for plotting the boundaries of constant gain margin and phase margin in a parameter plane [20]. The frequency independent GPMT is given in the form:

$$C_t(A, \phi) = Ae^{-j\phi}. \tag{4}$$

To find the controller parameters for a given value of gain margin A of the control system given in Fig. 1, one needs to set $\phi = 0$ in (4). On the other hand, setting $A = 1$ in (4), one can obtain the controller parameters for a given phase margin ϕ.

III. Stabilization Using Fractional-Order $\mathrm{PI}^{\lambda}\mathrm{D}^{\mu}$ Controller

Consider the unity feedback fractional-order control system shown in Fig. 1. The problem is to compute a set of FOPID controllers stabilizing the plant of (1). The output of the control system can be written as

$$y = \frac{G(s)C(s)C_t(A,\phi)}{1 + G(s)C(s)C_t(A,\phi)} r. \tag{5}$$

Definition 3.1: The denominator of (5) is described as *fractional-order characteristic equation* (FOCE) of the closed loop system. Putting (1), (3) and (4) into (5), the FOCE can be written as

$$P(s; k_p, k_i, k_d, \lambda, \mu) = \sum_{i=0}^{n} \Big[a_i s^{\alpha_i + \lambda} + Ae^{-j\phi} e^{-\theta s} b_i s^{\beta_i} \times (k_d s^{\mu+\lambda} + k_p s^{\lambda} + k_i) \Big]. \tag{6}$$

For a given FOPID controller parameters k_p, k_i, k_d, λ and μ the closed-loop system is said to be bounded-input bounded-output (BIBO) stable if the quasipolynomial $P(s; k_p, k_i, k_d, \lambda, \mu)$ has no roots in the closed right-half of the s-plane (RHP). The stability domain $\boldsymbol{S}$ in the parameter space $\boldsymbol{P}$ with k_p, k_i, k_d, λ and μ being coordinates is the region that for $(k_p, k_i, k_d, \lambda, \mu) \in \boldsymbol{S}$ the roots of quasi-polynomial $P(s; k_p, k_i, k_d, \lambda, \mu)$ all lie in open left-half of the s-plane (LHP). The boundaries of the stability domain $\boldsymbol{S}$ which are described by real root boundary (RRB), infinite root boundary (IRB) and complex root boundary (CRB) can be determined by the D-decomposition method [14], [21]. These boundaries are defined by the equations $P(0; \mathbf{k}) = 0$, $P(\infty; \mathbf{k}) = 0$ and $P(\pm \mathrm{j}\omega; \mathbf{k}) = 0$ for $\omega \in (0, \infty)$, respectively, where $P(s; \mathbf{k})$ is the characteristic function of the closed loop system and $\mathbf{k}$ is the vector of controller parameters.

In applying the descriptions of stability boundaries of the stability domain $\boldsymbol{S}$ to the FOCE in (6), the RRB turns out to be simply a straight line given by

$$P(0; k_p, k_i, k_d, \lambda, \mu) = b_i k_i = 0 \Leftrightarrow k_i = 0 \tag{7}$$

for $s^{\beta_0} = 1$ in the transfer function of the plant in (1).

There is more theoretical difficulties for the calculating of the IRB due to time delay. FOCE possesses an infinite number of roots, which can not be calculated analytically in the general case. However, the asymptotic location of roots far from the origin is well known [21], [22], which may lead to IRB. It can be shown in (6) that IRB only exist, if the degree equation $\alpha_n \leq \beta_n + \mu$ is fulfilled. In this case, the IRB can be described by the following equations:

$$k_d = \begin{cases} 0 & \text{for } (\alpha_n = \beta_n) \\ & \quad \text{or } (\alpha_n > \beta_n \text{ and } \mu > \alpha_n - \beta_n) \\ \pm a_n / b_n & \text{for } (\alpha_n > \beta_n \text{ and } \mu = \alpha_n - \beta_n) \\ \text{none} & \text{for } (\alpha_n > \beta_n \text{ and } \mu < \alpha_n - \beta_n). \end{cases} \tag{8}$$

To construct the CRB, we substitute $s = \mathrm{j}\omega$ into (6) to obtain

$$\begin{aligned} &P(\omega; k_p, k_i, k_d, \lambda, \mu) \\ &\quad = \sum_{i=0}^{n} \Big[a_i (j\omega)^{\alpha_i + \lambda} \Big] \\ &\qquad + \sum_{i=0}^{n} \Big[Ae^{-j(\omega\theta + \phi)} \Big(k_d b_i (j\omega)^{\beta_i + \mu + \lambda} \\ &\qquad\qquad + k_p b_i (j\omega)^{\beta_i + \lambda} + k_i b_i (j\omega)^{\beta_i} \Big) \Big] \\ &\quad = 0 \end{aligned} \tag{9}$$

The noninteger power of a complex number $(\sigma + j\omega)^{\gamma}$ can be calculated by

$$(\sigma + j\omega)^{\gamma} = \sqrt[\gamma]{\sigma^2 + \omega^2} \Big[\cos\Big(\gamma \tan^{-1} \frac{\omega}{\sigma} \Big) + j \sin\Big(\gamma \tan^{-1} \frac{\omega}{\sigma} \Big) \Big] \tag{10}$$

where σ is the real part, ω is the imaginary part and γ is the fractional order of the complex number. Using (10), the terms $j^{\alpha_i + \lambda}$, $j^{\beta_i + \mu + \lambda}$, $j^{\beta_i + \lambda}$, and j^{β_i}, which are required for (9) can be expressed as

$$\begin{aligned} j^{\alpha_i + \lambda} &= \cos\Big[(\alpha_i + \lambda) \frac{\pi}{2} \Big] + j \sin\Big[(\alpha_i + \lambda) \frac{\pi}{2} \Big] \\ &= x_i + j y_i, \end{aligned} \tag{11}$$

$$\begin{aligned} j^{\beta_i + \mu + \lambda} &= \cos\Big[(\beta_i + \mu + \lambda) \frac{\pi}{2} \Big] + j \sin\Big[(\beta_i + \mu + \lambda) \frac{\pi}{2} \Big] \\ &= z_i + j t_i \end{aligned} \tag{12}$$

$$\begin{aligned} j^{\beta_i + \lambda} &= \cos\Big[(\beta_i + \lambda) \frac{\pi}{2} \Big] + j \sin\Big[(\beta_i + \lambda) \frac{\pi}{2} \Big] \\ &= q_i + j r_i, \end{aligned} \tag{13}$$

$$j^{\beta_i} = \cos\Big(\beta_i \frac{\pi}{2} \Big) + j \sin\Big(\beta_i \frac{\pi}{2} \Big) = m_i + j l_i. \tag{14}$$

Hence, $P(\omega; k_p, k_i, k_d, \lambda, \mu)$ can be written as

$$\begin{aligned} &\sum_{i=0}^{n} \Big[a_i \omega^{\alpha_i + \lambda} (x_i + j y_i) + (A\cos(\omega\theta + \phi) - j \sin(\omega\theta + \phi)) Q_i \Big] \\ &\quad = \Re \{ P(\omega; k_p, k_i, k_d, \lambda, \mu) \} + j \Im \{ P(\omega; k_p, k_i, k_d, \lambda, \mu) \} \\ &\quad = 0 \end{aligned} \tag{15}$$

where

$$Q_i = k_d b_i \omega^{\beta_i+\mu+\lambda}(z_i + jt_i) + k_p b_i \omega^{\beta_i+\lambda}(q_i + jr_i) + k_i b_i \omega^{\beta_i}(m_i + jl_i).$$

Here, $\Re\{P(\omega; k_p, k_i, k_d, \lambda, \mu)\}$ and $\Im\{P(\omega; k_p, k_i, k_d, \lambda, \mu)\}$ denote the real and the imaginary parts of the FOCE, respectively. Then, equating the real and imaginary parts of (15) to zero, one obtains

$$\begin{aligned} k_p Z(\omega) + k_i Q(\omega) &= k_d K(\omega) + X(\omega) \\ k_p T(\omega) + k_i R(\omega) &= k_d L(\omega) + Y(\omega) \end{aligned} \tag{16}$$

where

$$Z(\omega) = \cos(\omega\theta + \phi)\sum_{i=0}^{n} b_i q_i \omega^{\beta_i+\lambda} + \sin(\omega\theta + \phi)\sum_{i=0}^{n} b_i r_i \omega^{\beta_i+\lambda} \tag{17a}$$

$$T(\omega) = \cos(\omega\theta + \phi)\sum_{i=0}^{n} b_i r_i \omega^{\beta_i+\lambda} - \sin(\omega\theta + \phi)\sum_{i=0}^{n} b_i q_i \omega^{\beta_i+\lambda} \tag{17b}$$

$$Q(\omega) = \cos(\omega\theta + \phi)\sum_{i=0}^{n} b_i m_i \omega^{\beta_i} + \sin(\omega\theta + \phi)\sum_{i=0}^{n} b_i l_i \omega^{\beta_i} \tag{17c}$$

$$R(\omega) = \cos(\omega\theta + \phi)\sum_{i=0}^{n} b_i l_i \omega^{\beta_i} - \sin(\omega\theta + \phi)\sum_{i=0}^{n} b_i m_i \omega^{\beta_i} \tag{17d}$$

$$K(\omega) = -\cos(\omega\theta + \phi)\sum_{i=0}^{n} b_i z_i \omega^{\beta_i+\mu+\lambda} - \sin(\omega\theta + \phi)\sum_{i=0}^{n} b_i t_i \omega^{\beta_i+\mu+\lambda} \tag{17e}$$

$$L(\omega) = -\cos(\omega\theta + \phi)\sum_{i=0}^{n} b_i t_i \omega^{\beta_i+\mu+\lambda} + \sin(\omega\theta + \phi)\sum_{i=0}^{n} b_i z_i \omega^{\beta_i+\mu+\lambda} \tag{17f}$$

$$X(\omega) = -(1/A)\sum_{i=0}^{n} a_i x_i \omega^{\alpha_i+\lambda}$$

$$\text{and } Y(\omega) = -(1/A)\sum_{i=0}^{n} a_i y_i \omega^{\alpha_i+\lambda}. \tag{17g}$$

Finally, by solving the 2-D system of (16) the k_p and k_i parameters in terms of k_d, λ and μ are obtained as

$$k_p = \frac{X(\omega)R(\omega) - Y(\omega)Q(\omega) + k_d(K(\omega)R(\omega) - L(\omega)Q(\omega))}{Z(\omega)R(\omega) - Q(\omega)T(\omega)} \tag{18}$$

$$k_i = \frac{Y(\omega)Z(\omega) - X(\omega)T(\omega) + k_d(L(\omega)Z(\omega) - K(\omega)T(\omega))}{Z(\omega)R(\omega) - Q(\omega)T(\omega).} \tag{19}$$

The above two equations trace out a curve in the (k_p, k_i)-plane representing the CRB, for fixed k_d, λ and μ, as ω runs from 0 to ∞.

Corollary 3.1: For $A = 1$ and $\phi = 0$, the stability boundaries RRB, IRB and CRB which divide the parameter space (k_p, k_i) into stable and unstable regions for the fixed values of k_d, λ and μ is determined. The stable region can be found by checking one arbitrary test point within each region. The characteristic equation belonging to the stable region has no RHP roots while the characteristic equation of the unstable region has a certain number of RHP roots. For checking the stability of the fractional-order characteristic equation, an effective numerical algorithm is given in [4]. The region having the stable characteristic equation, which is called the *general stability region*, gives a set of the stabilizing k_p and k_i parameters for the fixed values of k_d, λ and μ. It is noted that different choices of λ and μ lead to different general stability regions. By changing λ and μ in the range of (0, 2), the set of general stability regions is obtained. The values of λ and μ giving the biggest stability region are chosen. By sweeping over k_d for the specified values of λ and μ, a three-dimensional stability region, namely *global stability region*, for a given plant is obtained.

Corollary 3.2: Once the global stability region is obtained, a surface providing the specified values of gain margin or phase margin within this global stability region can be determined. This surface is called *local stability surface*. To find the controller parameters for a given value of gain margin A, one needs to set $\phi = 0$ in (18) and (19). On the other hand, setting $A = 1$ in (18) and (19), one can obtain the controller parameters for a given phase margin ϕ.

The presented stabilization algorithm for the FOPID controller is summarized as follows.

Step 1) Construction of the global stability region ($A = 1, \phi = 0$):
- ***1a***. Investigate the presences of RRB and IRB from (7) and (8)
- ***1b***. Use (18) and (19) to obtain the equations of k_p and k_i in terms of k_d, λ and μ for the CRB curve.
- ***1c***. For the fixed values of k_d, λ and μ;
  - — Obtain all regions by plotting the IRB line, RRB line and CRB curve in the same (k_p, k_i)-plane,
  - — Determine the general stability region by checking each region using the arbitrary test points.
- ***1d***. For a fixed value of k_d;
  - — Find the set of general stability regions by using different values of λ for the $\mathrm{PI}^{\lambda}\mathrm{D}$ controller ($\mu = 1$), and specify the value of λ which gives the biggest general stability region in this set.
  - — Find the set of general stability regions by using different values of μ for the PID^{μ} controller ($\lambda = 1$), and specify the value of μ which gives the biggest general stability region in this set.
- ***1e***. Plot the global stability region in the (k_p, k_i, k_d)-space for the specified values of λ and μ in Step 1d.

Step 2) Determination of the local stability surfaces for the prespecified values of A and ϕ:
- ***2a***. Obtain the set of controller parameters providing the desired value of gain margin for $\phi = 0$.
- ***2b***. Obtain the set of controller parameters providing the desired value of phase margin for $A = 1$.

A. Example 3.1

The fractional-order time delay system considered in [9] has the following transfer function

$$G(s) = \frac{1}{s^{1.5}} e^{-0.5s}. \tag{20}$$

The objective of the design is to investigate the global stability regions which make the closed loop characteristic equation stable. The FOCE of the control system for $A = 1$ and $\phi = 0$ is derived as

$$P(s) = s^{\lambda+1.5} + e^{-0.5s}(k_d s^{\lambda+\mu} + k_p s^{\lambda} + k_i). \tag{21}$$

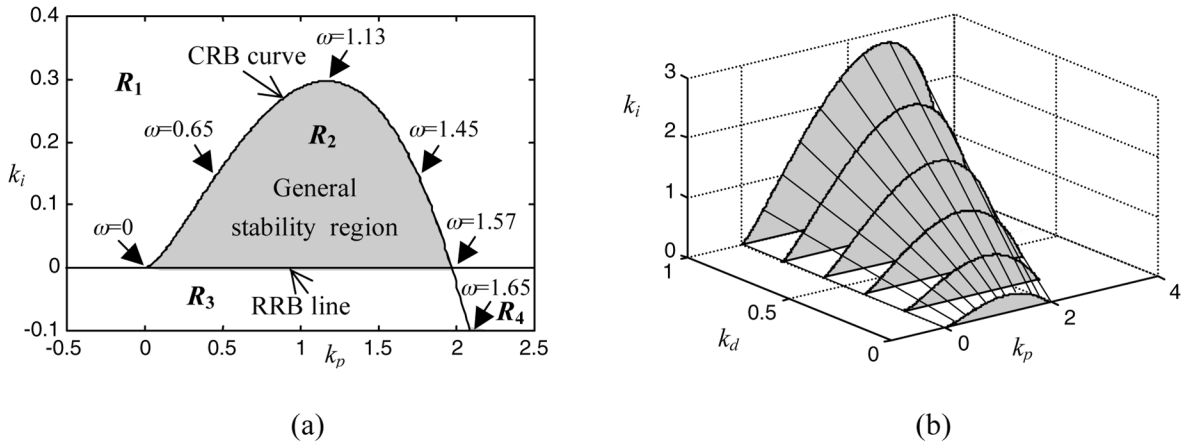

Fig. 2. (a) The general stability region for the PI controller ($k_d = 0, \lambda = 1, \mu = 1$). (b) The global stability region, which is composed of the general stability regions, for the PID controller ($\lambda = 1, \mu = 1$).

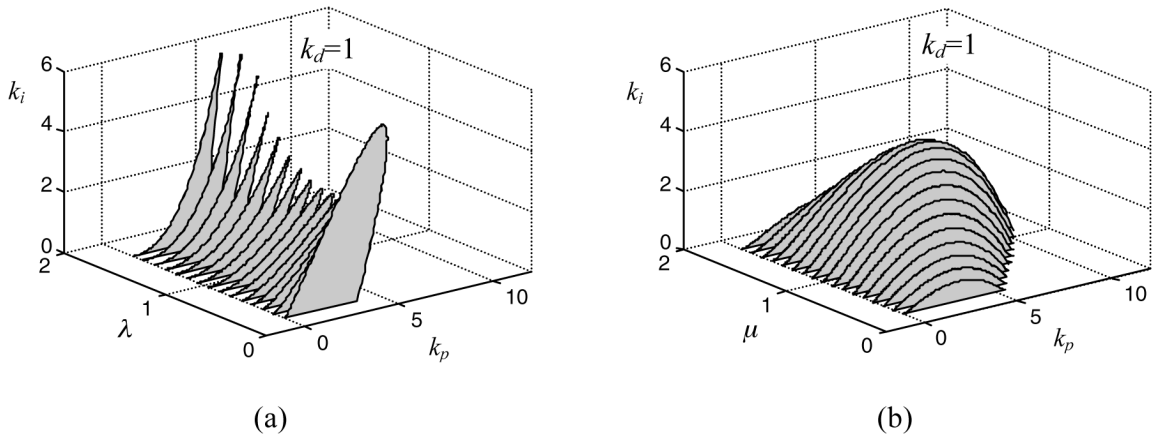

Fig. 3. The sets of general stability regions for the fractional-order controllers. (a) $\mathrm{PI}^{\lambda}\mathrm{D}$. (b) PID^{μ}.

The RRB and IRB lines can be obtained from (7) and (8)

$$\text{RRB line}: \quad k_i = 0 \quad \text{since } s^{\beta_0} = 1 \tag{22}$$

$$\text{IRB line}: \quad \begin{cases} k_d = 0 & \text{for } \mu > 1.5 \\ k_d = \pm 1 & \text{for } \mu = 1.5 \\ \text{none} & \text{for } \mu < 1.5 \end{cases}. \tag{23}$$

In order to get the CRB curve, it is made use of (18)-(19) so that we have (24)-(25) at the bottom of the page.

For the simplest case, i.e., $k_d = 0$ and $\lambda = \mu = 1$, the CRB curve and the RRB line are plotted in the (k_p, k_i)-plane as shown in Fig. 2(a). It can be observed from this figure that the parameter plane is divided into four regions, namely R_1, R_2, R_3 and R_4. By choosing one arbitrary test point in each regions and using the method in [4], the general stability region which is the shaded region (R_2) shown in Fig. 2(a) is determined. In this figure, the CRB curve is computed for the range of $\omega \in [0, 1.65]$. Equating (22)to (25), the intersection frequency is calculated as 1.57. By varying k_d and repeating the above procedure, different general stability regions are obtained for each k_d. The global stability region can then be visualized in a 3-D plot as shown in Fig. 2(b). From (23), the IRB does not exist and the global stability region has not an upper boundary in the k_d-axis. Therefore, k_d-axis is limited with an upper value $k_d = 1$ for good visibility. It is also seen from this figure that larger values of k_d provide bigger general stability regions, which means that the control system produces more various behaviors by increasing of the parameter k_d.

Choosing a k_d value, for example $k_d = 1$, from Fig. 2(b), the sets of the general stability regions computed by using different values of λ

$$k_p = -\frac{\omega^{\lambda+1.5}\sin\left[\omega\theta + \phi + (\lambda+1.5)\frac{\pi}{2}\right] + k_d A\omega^{\lambda+\mu}\sin\left[(\lambda+\mu)\frac{\pi}{2}\right]}{A\omega^{\lambda}\sin\left(\lambda\frac{\pi}{2}\right)} \tag{24}$$

$$k_i = \frac{\omega^{2\lambda+1.5}\sin[0.5\omega + \phi + 2.36] + k_d A\omega^{2\lambda+\mu}\sin\left(\mu\frac{\pi}{2}\right)}{A\omega^{\lambda}\sin\left(\lambda\frac{\pi}{2}\right)}. \tag{25}$$

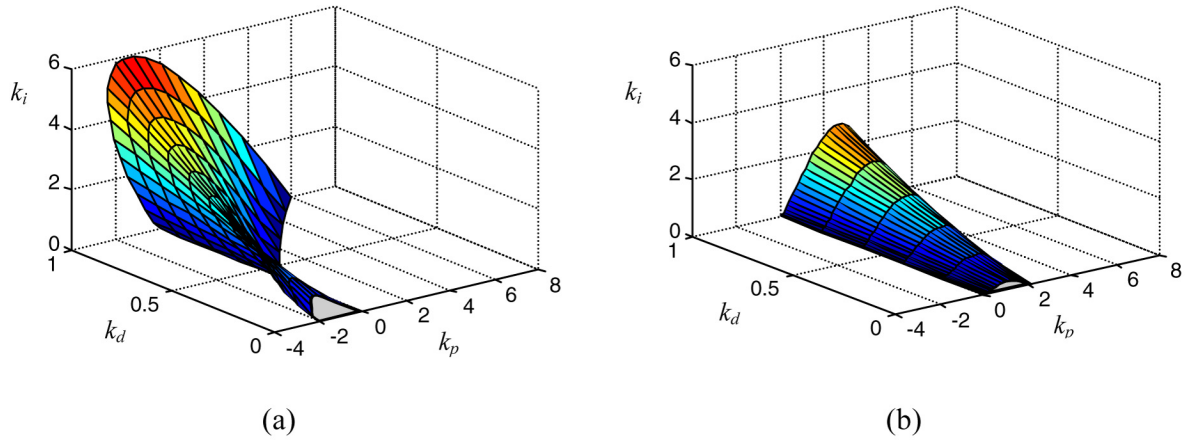

Fig. 4. The global stability regions (a) for the $\mathrm{PI}^{0.2}\mathrm{D}^{1.3}$ controller; (b) for the PID controller.

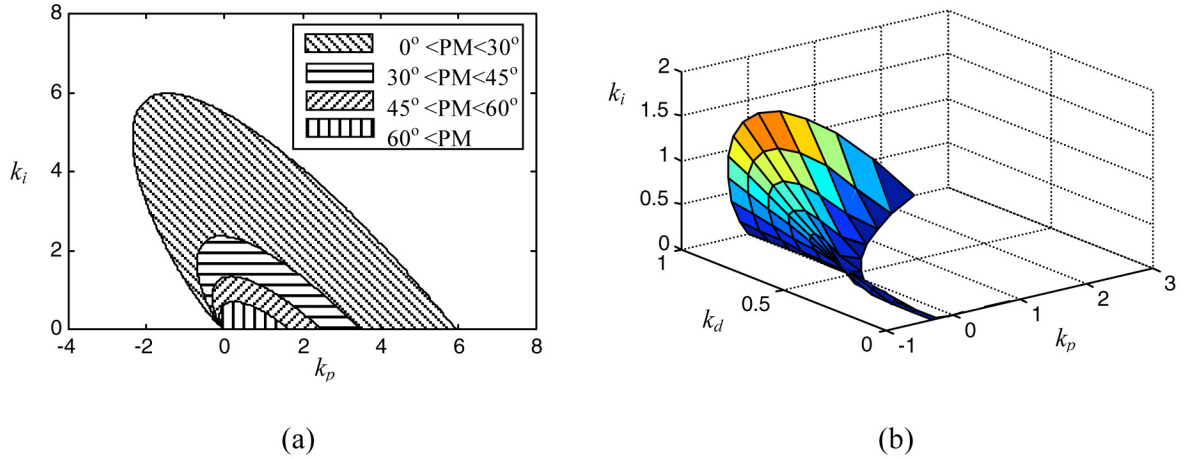

Fig. 5. (a) The general stability regions for some phase margins. (b) Local stability surface for $\phi = 45°$.

and μ for the $\mathrm{PI}^{\lambda}\mathrm{D}$ and PID^{μ} controllers are shown in Fig. (3a) and (b), respectively. In these figures, the values of λ and μ are taken in the range of [0.2, 1.7] for better visibility instead of (0, 2). Beyond these values, the general stability regions become very small for $\mu < 0.2$ and $\mu > 1.7$, and narrow decreasingly for $\lambda > 1.7$, and enlarge increasingly for $\lambda < 0.2$. In consideration of the range given for λ and μ, it is seen from these figures that the $\mathrm{PI}^{0.2}\mathrm{D}$ and $\mathrm{PID}^{1.3}$ controllers provide the biggest general stability regions. However, if both of Figs. (3a) and (b) are come together, then, it can be easily seen that the general stability region is not biggest for $\lambda = 1$ while the general stability region is the biggest for $\mu = 1.3$ for the $\mathrm{PID}^{1.3}$ controller. The same thing is also valid for the $\mathrm{PI}^{0.2}\mathrm{D}$ controller. Therefore, a balanced decision can be made for $\lambda = 0.2$ and $\mu = 1.3$ which gives the possible biggest global stability region for $\mathrm{PI}^{\lambda}\mathrm{D}^{\mu}$ controller. The global stability regions for fractional-order $\mathrm{PI}^{0.2}\mathrm{D}^{1.3}$ controller and integer-order PID controller are shown in Fig. 4. It can be seen from this figure that the FODIP controller has given bigger global stability region when compared with the classical PID controller.

After choosing the values of k_d, λ and μ, the local stability surfaces corresponding to the specified gain and phase margins can be obtained. For satisfactory performance, the gain margin should be greater than 2, and the phase margin should be between 30° and 60° [23]. Here, let us only consider the phase margin. The phase margin is more important specification than the gain margin for the system in (20) since it is closely related to overshoot [9]. The general stability regions for some specified phase margins can be determined for the $\mathrm{PI}^{0.2}\mathrm{D}^{1.3}$ controller by using the procedure given in Step 2.b as shown in Fig. 5(a). For a fixed value of phase margin, for example $\phi = 45°$, the local stability surface is shown in Fig. 5(b). As evidenced by the results given in this figure, it can be concluded that the proposed algorithm is reliable method not only for stabilizing of the FOTDS using FOPID controllers but also obtaining the set of FOPID controllers guarantying gain and phase margins.

IV. Conclusion

In this note, a useful stabilization method has been presented to obtain the stabilizing fractional-order $\mathrm{PI}^{\lambda}\mathrm{D}^{\mu}$ controllers for a given arbitrary fractional-order time delay system. The basis of this approach is to determine the stability domain boundaries via D-decomposition [14]. In this method, by using these boundaries the set of three-dimensional global stability regions in the parameter space is found since the fractional orders of the $\mathrm{PI}^{\lambda}\mathrm{D}^{\mu}$ controller can be changed in the range of (0, 2). This set includes all stabilizing $\mathrm{PI}^{\lambda}\mathrm{D}^{\mu}$ controllers for a given fractional-order time delay system. Choosing the biggest global stability region as shown in the example, the designer can make a decision for the selection of the $\mathrm{PI}^{\lambda}\mathrm{D}^{\mu}$ controller parameters. The method is also used to obtain the controllers that provide the desired gain and phase margins. Hence, a new set of the stabilizing $\mathrm{PI}^{\lambda}\mathrm{D}^{\mu}$ controllers within the global stability region are obtained. The part of the global stability region is called local stability surface. Numerical and graphical computation results have shown that the proposed approach has the

potential for analysis and design of very complicated fractional-order control systems with time delay.

The future direction in this research is to make more efforts on changing of the orders of FOPID controller. Furthermore, the choosing of the controller providing the optimal control in the global stability region can be investigated. To achieve this, it is needed to obtain the curves of the important time domain specifications such as settling time and maximum overshoot. Because the frequency and time domain performances will be met on a single plane, the designer can easily decide about choosing the controller parameters according to the desired performance.

REFERENCES

[1] K. J. Astrom and T. Hagglund, *Advanced PID Control*. Research T. Park, NC: ISA, 2005.

[2] M. Johnson, J. Croweand, and M. H. Moradi, *PID Control: New Identification and Design Methods*. London, U.K.: Springer, 2005.

[3] A. Datta, M.-T. Ho, and S. P. Bhattacharyya, *Structure and Synthesis of PID Controllers*. London, U.K.: Springer-Verlag, 2000.

[4] C. Hwang and Y.-C. Cheng, "A numerical algorithm for stability testing of fractional delay systems," *Automatica*, vol. 42, no. 5, pp. 825–831, 2006.

[5] I. Podlubny, "Fractional-order systems and $PI^{\lambda}D^{\mu}$-controllers," *IEEE Trans. Autom. Control*, vol. 44, no. 1, pp. 208–214, 1999.

[6] J. F. Leu, S. Y. Tsay, and C. Hwang, "Design of optimal fractional-order PID controllers," *J. Chinese Inst. Chem. Eng.*, vol. 33, no. 2, pp. 193–202, 2002.

[7] C. A. Monje, B. M. Vinagre, V. Feliu, and Y. Q. Chen, "On auto-tuning of fractional order $PI^{\lambda}D^{\mu}$ controllers," in *Proc. FDA 2006 Fractional Derivatives and Appl.*, Porto, Jul. 19–21, 2006.

[8] C. Hwang, J.-F. Leu, and S.-Y. Tsay, "A note on time-domain simulation of feedback fractional-order systems," *IEEE Trans. Autom. Control*, vol. 47, no. 4, pp. 625–631, 2002.

[9] S. Manabe, "Early development of fractional order control," in *Proc. ASME 2003 Design Eng. Tech. Conf.*, Chicago, IL, Sep. 2–6, 2003.

[10] G. J. Silva, A. Datta, and S. P. Bhattacharyya, "New results on the synthesis of PID controllers," *IEEE Trans. Autom. Control*, vol. 47, no. 2, pp. 241–252, 2002.

[11] N. Tan, "Computation of stabilizing lag/lead controller parameters," *Comp. Elect. Eng.*, vol. 29, pp. 835–849, 2003.

[12] M. T. Soylemez, N. Munro, and H. Baki, "Fast calculation of stabilizing PID controllers," *Automatica*, vol. 39, pp. 121–126, 2003.

[13] S. E. Hamamci and N. Tan, "Design of PI controllers for achieving time and frequency domain specifications simultaneously," *ISA Trans.*, vol. 45, no. 4, pp. 529–543, 2006.

[14] J. I. Neimark, "D-decomposition of the space of quasi-polynomials (on the stability of linearized distributive systems)," in *Amer. Math. Soc. (AMS) Transl.*, ser. 2. Providence, R. I.: AMS Soc., 1973, vol. 102, Ten papers in analysis, pp. 95–131.

[15] P. J. Lawrenson and S. R. Bowes, "Generalization of D-decomposition techniques," *Proc. Inst. Elect. Eng.*, vol. 116, pp. 1463–1470, 1969.

[16] J. McKay, "The D-partition method applied to systems with dead time and distributed lag," *Meas. Control*, vol. 3, pp. 293–294, 1970.

[17] S. L. Cheng and C. Hwang, "On stabilization of time-delay unstable systems using PID controllers," *J. Chinese Inst. Chem. Eng.*, vol. 30, no. 2, pp. 123–140, 1999.

[18] Y. M. Borushko and V. M. Vartanyan, "Automated synthesis of automated control systems using regions of specified quality," *Soviet J. Automation Inf. Sci.*, vol. 21, no. 3, pp. 64–66, 1988.

[19] A. T. Shenton and Z. Shafiei, "Relative stability for control systems with adjustable parameters," *J. Guid., Control, Dyn.*, vol. 17, pp. 304–310, 1994.

[20] C.-H. Chang and K.-W. Han, "Gain margins and phase margins for control systems with adjustable parameters," *J. Guid., Control, Dyn.*, vol. 13, no. 3, pp. 404–408, 1990.

[21] Y.-C. Cheng and C. Hwang, "Stabilization of unstable first-order time-delay systems using fractional-order PD controllers," *J. Chinese Inst. Eng.*, vol. 29, no. 2, pp. 241–249, 2006.

[22] R. E. Bellman and K. L. Cooke, *Differential-Difference Equations*. New York: Academic, 1963.

[23] K. Ogata, *Modern Control Engineering*. Englewood Cliffs, NJ: Prentice-Hall, 1970.

Optimal Signaling Policies for Decentralized Multicontroller Stabilizability Over Communication Channels

Serdar Yüksel and Tamer Başar

***Abstract*—In this note, we study the problem of distributed control over communication channels, where a number of distributed stations collaborate to stabilize a linear system. We quantify the rate requirements and obtain optimal signaling, coding and control schemes for decentralized stabilizability in such multicontroller systems. We show that in the absence of a centralized decoder at the plant, there is in general a rate loss in decentralized systems as compared to a centralized system. This result is in contrast with the absence of rate loss in the stabilization of multisensor systems. Furthermore, there is rate loss even if explicit channels are available between the stations. We obtain the minimum data rates needed in terms of the open-loop system matrix and the connectivity graph of the decentralized system, and obtain the optimal signaling policies. We also present constructions leading to stability. In addition, we show that if there are dedicated channels connecting the controllers, rate requirements become more lenient, and as a result strong connectivity is not required for decentralized stabilizability. We determine the minimum number of such external channels leading to a stable system, in case strong connectivity is absent.**

***Index Terms*—Cooperative control, decentralized stabilization, distributed control, information theory.**

I. INTRODUCTION AND LITERATURE REVIEW

Decentralization in control systems has become ubiquitous with the use of digital and wireless channels such as the Internet or dedicated bus lines [in a controller area network (CAN)] in control systems. Some typical applications include environmental detection, rescue operations, traffic management, formation control, and aerospace applications; see for instance [1]. In such remote control problems, one major concern is the characterization of the minimum amount of information transfer needed for a satisfactory performance. This information transfer could be between various components of a networked control system, as depicted in Fig. 1. Such networks and channels bring up many challenges, since they involve two disciplines which are still in their infancy, namely the decentralized control and the multiterminal information theories.

Decentralized stabilization has attracted considerable interest in the literature [2], [3]. One of the accomplishments in this domain is the introduction of *decentralized fixed modes* [4] and graph-theoretic characterization of stability [3] (see also [2]).

In distributed control problems, it is possible for the controllers to communicate through the plant [5]. The process of communicating via the plant is known as *signaling*. Most of the control literature on signaling is concerned with indirect aspects of signaling in optimal control

Manuscript received August 24, 2006; revised March 22, 2007, April 9, 2007, and May 14, 2007. Recommended by Associate Editor E. Jonckheere. The work of S. Yüksel was supported in part by the NSF under Grant CCR 00-85917 ITR. The work of T. Başar was supported in part by the NSF Grant CCR 00-85917 ITR.

S. Yüksel was with the University of Illinois at Urbana–Champaign, Urbana, IL 61801-2307 USA. He is now with the Mathematics and Engineering Program, Queen's University, Kingston, ON K7L 3N6, Canada. (e-mail: yuksel@mast.queensu.ca).

T. Başar is with the Coordinated Science Laboratory, University of Illinois at Urbana–Champaign, Urbana, IL 61801-2307 USA (e-mail: tbasar@decision.csl.uiuc.edu).

Digital Object Identifier 10.1109/TAC.2007.904279